Pramana – J. Phys. (2018) 91:87
https://doi.org/10.1007/s12043-018-1660-8

Shape, size and phonon scattering effect on the thermal conductivity of nanostructures

M GOYAL

Department of Physics, GLA University, Mathura 281 406, India
E-mail: monika.goyal@gla.ac.in

MS received 16 March 2018; revised 12 May 2018; accepted 15 May 2018; published online 13 October 2018

Abstract. A phenomological model is described here to study the effect of size, shape and phonon scattering on the thermal conductivity of nanostructures. Using the classical model proposed by Guisbiers *et al* (*Phys. Chem. Chem. Phys.* **12**, 7203 (2010), *J. Phys. Chem. C* **112**, 4097 (2008)) in terms of the melting temperature of nanostructures, the expression for variation of thermal conductivity is obtained in terms of shape and size parameter. An additional term is included in the expression of thermal conductivity to consider the impact of phonon scattering due to the surface roughness with a decrease in size. The expression of thermal conductivity is obtained for spherical nanosolids, nanowires and nanofilms. The thermal conductivity is found to decrease in nanostructures in comparison with the counterpart bulk material. The values of thermal conductivity obtained from the present model are found to be close to the available experimental data for different values of roughness parameter which verifies the suitability of the model.

Keywords. Nanomaterials; shape factor; size effect; roughness parameter; thermal conductivity.

PACS Nos 65.80.+n; 72.20.−i

1. Introduction

The study carried out to understand the heat conduction and thermal transport mechanism in semiconductors has been of great scientific interest because of its worldwide applications in thermoelectric and optoelectronic devices [1–3]. The phenomenon of heat transport is dominated by phonons in bulk semiconductors and results in excellent thermal properties. The thermal transport properties of nanomaterials are also important to study the development of nanoscale electronic devices. Various methods have been applied by scientists to understand the physical, optical, electronic properties of nanomaterials and the practical applications of nanodevices [4–7]. Experimental as well as theoretical investigations are performed to study the thermal properties of pure semiconductors, semiconductor alloys and their superlattices. The efficiency of thermoelectric modules depends on the thermoelectric figure of merit (ZT) of its components. ZT depends on the Seeback coefficient, electrical resistivity and thermal conductivity. For nanostructured materials, the reduction in thermal conductivity contributes to the improvement in the figure of merit [8–11]. The thermal conductivity in nanoscale semiconducting systems is found to vary with reduction in size and is found to be smaller in nanomaterials than in the bulk form of the same material. These studies explain that the thermal transport properties in nanomaterials are different from that of their bulk form due to a decrease in size and quantum confinement, an increase in surface area-to-volume ratio in nanomaterials and reduction in phonon transport due to the scattering contribution [12–14]. Theoretical models that include the shape, size and scattering effect are still lacking, and so there is a need for a better theoretical model to explain the experimental results well at room temperature. In the present work, we have applied a phenomenological model based on classical thermodynamics to analyse the variation in thermal conductivity of nanostructures in comparison with the bulk with respect to size [15–17]. The mathematical formulation is presented in §2 and the results obtained from the present approach are discussed in §3.

2. Mathematical formulations

Using the energy conservation law and concept of classical thermodynamics for a nanostructure, the

melting temperature of a nanostructure is expressed as follows [17,18]:

$$\frac{T_{\mathrm{mN}}}{T_{\mathrm{m},\infty}} = 1 + \frac{(\gamma_{\mathrm{L}} - \gamma_S)\, A}{\Delta H_{\mathrm{m},\infty} V}, \tag{1}$$

where T_{mN} and $T_{\mathrm{m},\infty}$ are the melting temperatures of the nanostructure and its bulk form in Kelvin, respectively. γ_{L} is the surface energy in the liquid phase, γ_{S} is the surface energy in the solid phase and $\Delta H_{\mathrm{m},\infty}$ is the melting enthalpy for the bulk material. The surface area-to-volume ratio is represented by A/V.

Guisbiers *et al* [17,18] have expressed the melting temperature as a function of shape and size parameters for free-standing nanostructures as follows:

$$\frac{T_{\mathrm{m}}}{T_{\mathrm{m},\infty}} = 1 - \frac{\alpha_{\mathrm{shape}}}{D}. \tag{2}$$

D represents the diameter of the spherical nanostructure or size in the case of the non-spherical nanostructure, α_{shape} represents the shape-dependent parameter and it is clear from eq. (1) that it depends on γ_{L}, γ_{S} and $\Delta H_{\mathrm{m},\infty}$ [19,20]. The ratio A/V is expressed as a function of $1/D$.

The melting temperature of the bulk material is related to the cohesive energy [21] as follows:

$$T_{\mathrm{m},\infty} = \frac{0.032}{k_{\mathrm{B}}} E_0, \tag{3}$$

where k_{B} represents the Boltzmann constant.

Using eqs (2) and (3), the cohesive energy of the nanosolid E_{mN} and its bulk form E_0 are related as follows:

$$E_{\mathrm{mN}} = E_0\left(1 - \frac{\alpha_{\mathrm{shape}}}{D}\right). \tag{4}$$

The melting temperature T_{m} and the Debye temperature θ_{D} are related in accordance with the Lindemann criterion of melting [22,23] as follows:

$$\theta_{\mathrm{D}} = C\left(\frac{T_{\mathrm{m}}}{M V^{2/3}}\right)^{1/2}, \tag{5}$$

where C is a constant.

Therefore, θ_{D} has a square-root dependence on the melting temperature, i.e.

$$\theta_{\mathrm{D}} \propto (T_{\mathrm{m}})^{1/2}. \tag{6}$$

Considering eqs (2) and (6), the Debye temperature in nanosolids θ_{DN} is related to the Debye temperature in bulk θ_{DB} as follows

$$\theta_{\mathrm{DN}} = \theta_{\mathrm{DB}}\left(1 - \frac{\alpha_{\mathrm{shape}}}{\mathrm{D}}\right)^{1/2}. \tag{7}$$

The thermal conductivity of the bulk solid material k_{B} is given by [24]

$$k_{\mathrm{B}} = \frac{1}{3} C_{p\mathrm{B}}\, v_{\mathrm{P}} l_{\mathrm{o}}, \tag{8}$$

where $C_{p\mathrm{B}}$ is the specific heat, v_{P} is the average velocity of the phonon and l_{o} is the mean-free path of the bulk material.

The Debye temperature varies with the average phonon velocity [25,26] according to the relation

$$\theta_{\mathrm{D}} \propto \frac{2h}{\pi k_{\mathrm{B}}} \left(\frac{3N_A}{4\pi V}\right)^{1/3} v_{\mathrm{P}}, \tag{9}$$

where h is the Planck's constant, N_{A} is the Avagradro number, V is the molar volume and k_{B} is the Boltzmann's constant.

The Debye temperature of a nanomaterial and its bulk form are related to the average phonon velocity of a nanoparticle v_{N} and its bulk form v_{P} as follows:

$$\frac{\theta_{\mathrm{DN}}}{\theta_{\mathrm{DB}}} = \frac{v_{\mathrm{N}}}{v_{\mathrm{P}}}. \tag{10}$$

The mean-free path of the nanomaterial l_{N} and its bulk form l_{o} are related to the melting temperature and Debye temperature as follows [24,27]:

$$\frac{l_{\mathrm{N}}}{l_{\mathrm{o}}} = \frac{T_{\mathrm{mN}}}{T_{\mathrm{mB}}} = \frac{\theta_{\mathrm{DN}}^2}{\theta_{\mathrm{DB}}^2}. \tag{11}$$

The specific heat is considered to be constant for the bulk and nanomaterials at room temperature.

Therefore, the thermal conductivity of the nanomaterials and their bulk form are related as follows:

$$\frac{k_{\mathrm{N}}}{k_{\mathrm{B}}} = \frac{v_{\mathrm{N}} l_{\mathrm{N}}}{v_{\mathrm{P}} l_{\mathrm{o}}} = \frac{\theta_{\mathrm{DB}}^3}{\theta_{\mathrm{DN}}^3} = \left(1 - \frac{\alpha_{\mathrm{shape}}}{D}\right)^{3/2}. \tag{12}$$

The thermal conductivity of spherical nanosolids and nanowires of diameter D and nanofilms of height D is given by

$$\frac{k_{\mathrm{N}}}{k_{\mathrm{B}}} = \left(1 - \frac{\alpha_{\mathrm{sphere}}}{D}\right)^{3/2}, \tag{13}$$

$$\frac{k_{\mathrm{N}}}{\mathrm{k_B}} = \left(1 - \frac{\alpha_{\mathrm{nanowire}}}{D}\right)^{3/2}, \tag{14}$$

$$\frac{k_{\mathrm{N}}}{k_{\mathrm{B}}} = \left(1 - \frac{\alpha_{\mathrm{nanofilm}}}{D}\right)^{3/2}. \tag{15}$$

Equations (13)–(15) explain the thermal conductivity variation in nanomaterials with size.

With a decrease in size in the nanomaterials, the surface atom-to-volume ratio increases that causes large surface scattering due to more phonon–phonon interaction which in turn affects the heat transfer process in nanostructures. The phonon scattering at the interfaces varies with the surface roughness due to a decrease in size and this leads to non-equilibrium phonon distribution. The surface roughness and phonon scattering suppress the conduction in nanomaterials exponentially in comparison with their bulk form [6, 24,28]. So, a pre-term $p\exp(-l_{\mathrm{o}}/D)$ is included in the

expression of thermal conductivity, where p represents the surface roughness parameter and has a value between $0 < p \leq 1$. (l_o/D) is known as the Knudsen number, where l_o represents the phonon mean-free path at room temperature and D represents the diameter of the spherical nanoparticle and nanowire or height of the nanofilm. The large value of p corresponds to the smooth surface and therefore more probability of specular scattering and less diffusive scattering, whereas the small value of p corresponds to the rough surface and therefore more probability of diffusive scattering resulting in more decrease in thermal conductivity. Including phonon scattering effect, the expressions of thermal conductivity in spherical nanosolids, nanowires and nanofilms with respect to the thermal conductivity of bulk are as follows:

$$\frac{k_N}{k_B} = p\exp(-l_o/D)\left(1-\frac{\alpha_{sphere}}{D}\right)^{3/2}, \tag{16}$$

$$\frac{k_N}{k_B} = p\exp(-l_o/D)\left(1-\frac{\alpha_{nanowire}}{D}\right)^{3/2}, \tag{17}$$

$$\frac{k_N}{k_B} = p\exp(-l_o/D)\left(1-\frac{\alpha_{nanofilm}}{D}\right)^{3/2}. \tag{18}$$

The shape parameter for spherical nanoparticle, cylindrical nanowire and cylindrical nanofilm is in the ratio 3:2:1 [19].

3. Results and discussion

The model proposed in the present work considers the effect of size on mean-free path, phonon velocity and phonon scattering. The input values of the shape parameter and mean-free path are required for calculations at room temperature and these parameters are listed in table 1. The relative change in thermal conductivity of Si and GaAs nanostructures with size is observed using eqs (16)–(18) for spherical nanocrystals, nanowires and nanofilms. The thermal conductivity is considered to vary with D, the diameter or height of the nanostructure along with the surface roughness parameter p. The value of p lies between $0 < p \leq 1$. The roughness parameter is predicted to be 0.1, 0.4 and 0.8 for Si nanostructures. The calculated results from the present model are shown in figures 1a–1c for Si nanostructures. The roughness parameter p is taken to be 0.1, 0.3, 0.6 and 0.9 for GaAs nanostructures and the results obtained using the model are depicted in figures 2a–2c. The experimental results available for Si and GaAs nanostructures are also shown in figures 1 and 2 along with the present calculated values for comparison. The phenomological model predicts the thermal conductivity variation in nanostructures with size. When the size of the nanomaterial decreases, the thermal conductivity decreases in nanostructures. Also, with reduction in size, the value of the term $\exp(-l_o/D)$ decreases which corresponds to more interface scattering and reduction in heat conduction and thus reduced conductivity in nanosystems. For large values of p, the diffusive scattering is less whereas for small values of p, there is more probability of diffusive scattering which in turn affects the thermal conductivity. So, the present model explains the variation in thermal conductivity in nanostructures of different size and shape along with the phonon scattering effect on them. The shape parameters $\alpha_{nanofilm}/\alpha_{sphere}$ are in the ratio 1/3 and $\alpha_{nanowire}/\alpha_{sphere}$ are in the ratio 2/3 [18,19].

Figure 1a shows the variation in thermal conductivity of Si nanoparticles of different diameters with respect to their bulk form k_N/k_B at room temperature for roughness parameter $p = 0.1$, 0.4 and 0.8. For a small value of p, there is more reduction in thermal conductivity as it corresponds to much rougher surface while a larger value of p ($p \rightarrow \leq 1$), corresponds to smoother surface and a less decrease in thermal conductivity. Also, the thermal conductivity decreases with decrease in diameter or height (thickness) of the nanostructure as shown in the figure. Figure 1b shows the relative change in thermal conductivity with diameter for Si nanowires. The experimental data [29] available for Si nanowires at 300 K are found to be close to the predicted values of thermal conductivity from the present model for $p = 0.4$. Figure 1c shows the relative change in thermal conductivity k_N/k_B of Si nanofilms with size and the results are compared with the available experimental data [9,30] at room temperature. Good agreement of the present calculated results for $p = 0.8$ is observed with the available previous results [9,30] for Si nanofilms along the plane of the semiconductor.

Figures 2a and 2b show the relative change in thermal conductivity with diameter of GaAs spherical nanoparticles and nanowires at room temperature for roughness

Table 1. Input parameters [13,18,31].

No.	Semiconductor	l_o (nm)	α_{sphere} (nm)	$\alpha_{nanowire}$ (nm)	$\alpha_{nanofilm}$ (nm)	k_B (W/mK)
1	Si	41	1.16	0.78	0.39	148
2	GaAs	5.8	1.60	1.08	0.54	46

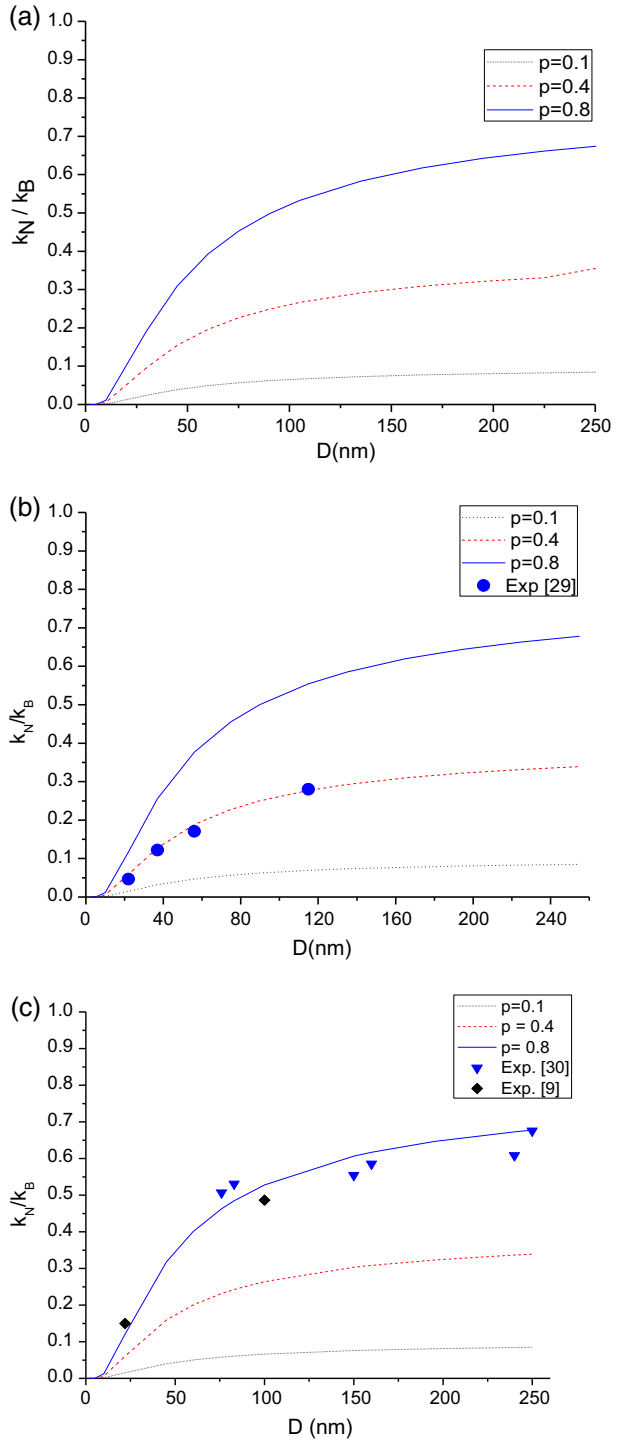

Figure 1. (**a**) Relative variation in thermal conductivity k_N/k_B with diameter D in Si spherical nanoparticles, (**b**) relative variation in thermal conductivity k_N/k_B with diameter D in Si cylindrical nanowires and (**c**) relative variation in thermal conductivity k_N/k_B with thickness D in Si nanofilms.

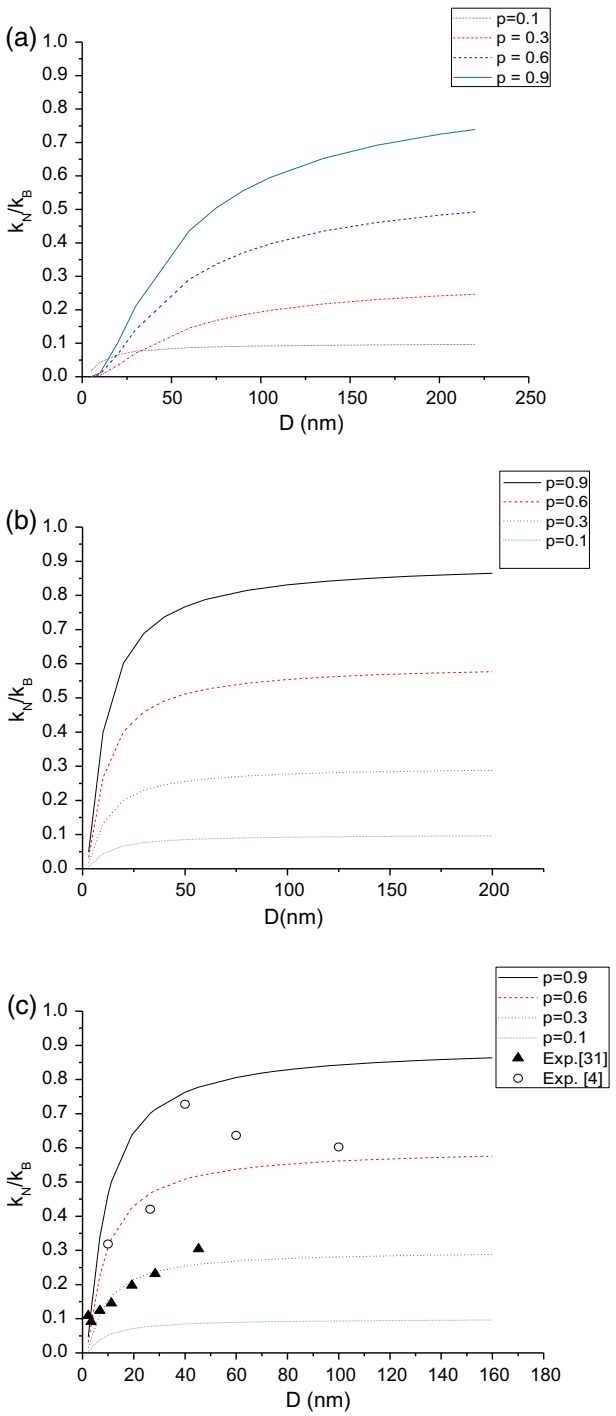

Figure 2. (**a**) Relative variation in thermal conductivity k_N/k_B with diameter D in GaAs spherical nanoparticles, (**b**) relative variation in thermal conductivity k_N/k_B with diameter D in GaAs cylindrical nanowires and (**c**) relative variation in thermal conductivity k_N/k_B with thickness D in GaAs nanofilms.

parameter $p = 0.1, 0.3, 0.6$ and 0.9. Figure 2c shows the calculated results for GaAs nanofilms and the results are compared with the available experimental results [4,31]. The open circles are experimental results [4] of thermal conductivity variation for GaAs/AlAs superlattices with thickness of 10–100 nm along the plane. The

present predicted results for $p = 0.6$ are close to the experimental data [4]. The triangles represent the experimental data [31] of thermal conductivity variation for GaAs/AlAs superlattices having thickness in the range 5–45 nm in perpendicular direction to its plane. The experimental results [31] are found to be in close agreement with the present calculated results for $p = 0.3$. The thermal conductivity is found to be least in spherical nanoparticles, whereas the thermal conductivity of nanofilms is more than that of the nanowires. It is thus evident from the results that the thermal conductivity is reduced in nanostructures in comparison with the counterpart bulk material at room temperature. Good consistency between the present calculated results and the available experimental values supports the suitability of the present model theory.

4. Conclusion

The theoretical model proposed in the present study can explain the variation in thermal conductivity in nanostructured semiconductors with reduction in size and surface scattering. It is important to mention here that both the size and shape influence the heat conduction mechanism of the nanostructure. From the overall analysis, it is noted that the thermal conductivity of nanofilms is more than that of the nanowires and spherical nanoparticles. As the present model successfully explains the variation in thermal conductivity in nanostructures with size, it may be useful for researchers engaged in exploring the thermal transport properties of nanoscale materials.

References

[1] C Weisbuch and B Vinter, *Quantum semiconductor structures* (Academic Press, San Diego, CA, 1991)
[2] A Yariv, *Quantum electronics*, 3rd edn (Wiley, New York, 1989)
[3] R J Moitsheki and C Harley, *Pramana – J. Phys.* **77**, 519 (2011)
[4] T Yao, *Appl. Phys. Lett.* **51(22)**, 1798 (1987)
[5] W S Capinski and H J Maris, *Physica B* **219–220**, 699 (1996)
[6] E Ziambaras and P Hyldgaard, *J. Appl. Phys.* **99**, 054303 (2006)
[7] M Malligavathy, S Iyyapushpam, S T Nishanthi and D Pathinettam Paditan, *Pramana – J. Phys.* **90**: 44 (2018)
[8] Y He and G Galli, *Phys. Rev. Lett.* **108**, 215901 (2012)
[9] W Liu and M Asheghi, *Appl. Phys. Lett.* **84**, 3819 (2004)
[10] Z Wang and N Mingo, *Appl. Phys. Lett.* **97**, 101903 (2010)
[11] C Q Sun, L K Pan, C M Li and S Li, *Phys. Rev. B* **72**, 134301 (2005)
[12] A Malhotra and M Maldovan, *J. Appl. Phys.* **120**, 204305 (2016)
[13] L H Liang and B Li, *Phys. Rev. B* **73**, 153303 (2006)
[14] D G Cahill, P V Braun, G Chen, D R Clarke, S Fan, K E Goodson, P Keblinski, W P King, G D Mahan, A Majumdar, H J Maris, S R Phillpot, E Pop and L Shi, *Appl. Phys. Rev.* **1**, 011305 (2014)
[15] G Guisbiers, *Nanoscale Res. Lett.* **5**, 1132 (2010)
[16] G Guisbiers and L Buchaillot, *Phys. Lett. A* **374**, 305 (2009)
[17] G Guisbiers, D Liu, Q Jiang and L Buchaillot, *Phys. Chem. Chem. Phys.* **12**, 7203 (2010)
[18] G Guisbiers, M Kazan, O V Overschelde, M Wautelet and S Pereira, *J. Phys. Chem. C* **112**, 4097 (2008)
[19] M Wautelet, *Phys. Lett. A* **246**, 341 (1998)
[20] G Guisbiers and M José-Yacaman, *Encyclopedia of interfacial chemistry: Surface science and electrochemistry*, in: Reference module in chemistry, molecular sciences and chemical engineering (Elsevier, New York, 2018) pp. 875–885
[21] J Ferrante, J H Rose and J R Smith, *Appl. Phys. Lett.* **44**, 53 (1984)
[22] F A Lindemann, *Phys. Z.* **11**, 609 (1910)
[23] J G Dash, *Rev. Mod. Phys.* **71**, 1737 (1999)
[24] J M Zimann, *Electrons and phonons* (Clarendon Press, Oxford, 1960), pp. 288, 58, 296, 456
[25] E J Post, *Can. J. Chem.* **31**, 112 (1953)
[26] A R Regal and V M Glazov, *Semiconductors* **29(5)**, 405 (1995)
[27] G Soyez, J A Eastman, L J Thompson, G R Bai, P M Baldo and A W McCormick, *Appl. Phys. Lett.* **77**, 1155 (2000)
[28] J Lim, K Hippalgaonkar, S C Andrews, A Majumdar and P Yang, *Nano Lett.* **12**, 2475 (2012)
[29] D Li, Y Wu, P Kim, L Shi, P Yang and A Majumdar, *Appl. Phys. Lett.* **83**, 3186 (2003)
[30] Y S Ju and K E Goodson, *Appl. Phys. Lett.* **74(20)**, 3005 (1999)
[31] W S Capinski, H J Maris, T Ruf, M Cardona, K Ploog and D S Katzer, *Phys. Rev. B* **59**, 8105 (1999)